

A Density Functional Theory Analysis of Electrochemical Oxidation of Methane to Alcohol over High-Entropy Oxide (CoCrFeMnNi)₃O₄ Catalysts

M. R. Ashwin Kishore,^[a] Sungwoo Lee,^[a] and Jong Suk Yoo*^[a]

(Special Collection Dedicated to Jens Nørskov).

The direct conversion of methane into alcohol is a promising approach for achieving a low-carbon future, yet it remains a major challenge. In this study, we utilize density functional theory to explore the potential of the (CoCrFeMnNi)₃O₄ (CCFMNO) high entropy oxide (HEO) for electrochemical oxidation of methane to methanol and ethanol, alongside their competition with CO₂ production. Our primary focus in this study is on thermodynamics, enabling a prompt analysis of the catalyst's potential, with the calculation of electrochemical barriers falling beyond our scope. Among all potential active

sites within CCFMNO HEO, we identify Co as the most active site for methane activation when using carbonate ions as oxidants. This results in methanol production with a limiting potential of 1.4 V_{CHE}, and ethanol and CO₂ productions with a limiting potential of 1.2 V_{CHE}. Additionally, our findings suggest that the occupied p-band center of O* on CCFMNO HEO is a potential descriptor for identifying the most active site within CCFMNO HEO. Overall, our results indicate that CCFMNO HEO holds promise as catalysts for methane oxidation to alcohols, employing carbonate ions as oxidants.

Introduction

Methane has significantly contributed to meeting global energy demands owing to its abundance and environmental advantages over conventional fossil fuels.^[1,2] Nevertheless, the current challenges associated with storing and transporting methane gas, particularly when produced at oil production sites, have led to extensive gas flaring in oil fields around the world. The direct conversion of methane through thermal catalysis is inefficient, lacks selectivity, and demands the use of strong reactants and harsh conditions (such as high temperatures and pressures), making methane conversion at remote locations highly challenging. Furthermore, these conditions generally favor complete oxidation over partial oxidation thermodynamically. An attractive alternative involves using electrocatalysis to partially oxidize methane to alcohol, employing a suitable catalyst and oxidant.

High-entropy alloys (HEAs) have recently emerged as attractive catalysts for various catalytic applications, including oxygen reduction reaction (ORR),^[3–5] oxygen evolution reaction (OER),^[4,6] CO oxidation,^[7] hydrogen evolution,^[8] ammonia

oxidation^[9] and decomposition,^[10] methanol oxidation,^[11,12] and carbon dioxide reduction reactions (CO₂RR).^[13,14] HEAs are composed of five or more elements arranged in a random order, resulting in a surface with multiple unique active sites.^[15] The interaction between the catalytic active site and adsorbate not only depends on the constituent elements but also on the surrounding environment, which includes adjacent atoms both laterally and beneath the surface. Consequently, modifying the alloy composition becomes a crucial strategy to fine-tune their catalytic behavior.^[16]

The concept of high-entropy stabilized alloys has been extended to oxides to exploit their intriguing properties.^[17] Among the extensively studied multinary transition metal high-entropy alloys is the Cr–Mn–Fe–Co–Ni alloy, often referred to as the “Cantor alloy,” demonstrating a single solid solution phase under various conditions.^[18–21] An oxide variant derived from this alloy, namely the (CoCrFeMnNi)₃O₄ high-entropy oxide and exhibits promising catalytic activity in diverse electrochemical applications. For instance, Triolo *et al.* demonstrated the potential of (Cr_{0.5}Mn_{0.5}Fe_{0.5}Co_{0.5}Ni_{0.5})₃O₄ HEOs as a promising catalyst for OER,^[22,23] while Sun *et al.* revealed exceptional Li⁺-storage capabilities in (Cr_{0.2}Mn_{0.2}Fe_{0.2}Co_{0.2}Ni_{0.2})₃O₄ HEOs powders.^[24] Furthermore, a mesoporous thin film of (Cr_{0.2}Mn_{0.2}Fe_{0.2}Co_{0.2}Ni_{0.2})₃O₄ HEOs has exhibited superior performance compared to a dense film, highlighting its potential as a photoelectrode for solar water reduction in alkaline media.^[25] Its inherent stability and unique compositional structure make it an attractive candidate for exploring its role in catalysis, particularly in electrochemical applications.

While the potential applications of HEOs in various catalytic processes have been widely explored,^[26] their utilization in electrochemical partial methane oxidation remains significantly

[a] Dr. M. R. A. Kishore, S. Lee, Prof. J. S. Yoo
Department of Chemical Engineering
University of Seoul
Seoul, 02504, Republic of Korea
E-mail: jsyoo84@uos.ac.kr

Supporting information for this article is available on the WWW under <https://doi.org/10.1002/cphc.202400098>

© 2024 The Authors. ChemPhysChem published by Wiley-VCH GmbH. This is an open access article under the terms of the Creative Commons Attribution Non-Commercial NoDerivs License, which permits use and distribution in any medium, provided the original work is properly cited, the use is non-commercial and no modifications or adaptations are made.

unexplored. A particular study primarily focused on the thermal oxidation of methane employing various HEOs supported on Cu, such as (MgNiZnCuCo) O_x , (MgTiZnCuCo) O_x , (AlFeCrGaTi) O_x , (FeCoMgNiMn) O_x , and (MgCaNiCoFeMn) O_x . However, this investigation encountered challenges in partially oxidizing methane, resulting in the production of CO₂ and CO within the temperature range of 200–500 °C. The limitations posed by thermal catalysis on HEOs could potentially be addressed through electrocatalysis. Hence, this study aims to delve into the potential of the equimolar face-centered cubic (CoCrFeMnNi)₃O₄ as a catalyst for electrochemical methane oxidation towards alcohol production.

In this study, we employ density functional theory (DFT) to investigate the electrochemical methane oxidation on the (CoCrFeMnNi)₃O₄ (CCFMNO) HEO, employing CO₃²⁻ ions as oxidant. Our reaction energetics analysis indicates that CCFMNO HEO has the capability to produce alcohols, with a slightly stronger preference for ethanol over methanol, alongside the production of CO₂ gas. Moreover, our investigation into the electronic structure of CCFMNO HEO revealed correlations between proton affinity and occupied p-band center of O*, emerged as a promising electronic descriptor for catalytic activity. This findings emphasizes its crucial role in future catalyst design strategies for methane conversion.

Results and Discussion

Generation of Active Oxygen Species on Catalyst Surface

An equimolar face-centered cubic high-entropy oxide comprising of Cr, Mn, Fe, Co, Ni were modeled using the special-quasirandom structure (SQS) of 5×5×4 supercells containing 100 atoms. The mcsqs code in the Alloy Theoretic Automated Toolkit (ATAT) was used to find the best SQS that most satisfies the correlation function of random solutions.^[27] It was found that the homogeneously mixed CCFMNO HEO bulk structure exhibits superior stability, and the optimized structure is shown in Figure S1. Next, we identified the relevant catalyst surface by examining different terminations of the (001) facet. The most stable surface termination included all active elements—cobalt, chromium, iron, manganese, and nickel—consistent with the homogeneous mixing observed in the bulk structure.

To further validate the presence of the most active element, Co, on the CCFMNO HEO surface, we conducted a comparative investigation by exchanging the position of the surface Co atom with either Cr, Fe or Mn in the subsurface. Our findings revealed that the total energies for Co on the surface are 4.3 meV, 19.4 meV, and 447.8 meV lower than those for Cr, Fe, and Mn on the surface, respectively.

To address potential composition variations between surface and bulk of HEOs in experiments, we delved into a scenario where cobalt, the most active element, forms a separate oxide phase (Co₃O₄). Our analysis, as depicted in Figure S2, indicates that the catalytic performance of Co₃O₄ is expected to be significantly inferior to that of our HEO due to a notably increased activation barrier for C–H activation of methane. This

highlights the importance of employing a catalyst comprising homogeneously mixed HEOs rather than having specific oxides predominant on the surface. The Pourbaix diagram for various metallic sites within CCFMNO HEO indicates that at pH=0, the clean surface remains stable up to 1.0 V_{RHE} without any pre-covered adsorbates, as shown in Figure 1. However, at potentials higher than 1.0 V_{RHE} and 1.37 V_{RHE}, the Cr and Ni sites, respectively, become poisoned by *O electrochemically formed via water oxidation. Subsequently, as the potential increases beyond 1.5 V_{RHE}, all metallic sites in CCFMNO HEO starts to be poisoned by O*. Therefore, under the experimental applied potentials for methane activation, typically falling within the range of 1.0 to 1.5 V_{RHE}, only the Co and Fe sites remain clean, while the Ni and Cr sites are occupied by O*.

In the electrochemical conversion of methane, the presence of active oxygen (O*) is crucial for effectively activating the C–H bond. As previously reported, the generation of O* on a catalyst surface using CO₃²⁻ ions is far more appealing compared to H₂O.^[28–30] The CO₃²⁻ ion as oxidant facilitates the generation of active atomic oxygen on the catalyst surface through the following reactions:



Equations (1) and (2) depict the electrochemical adsorption of a carbonate ion to CO₃* and the subsequent thermochemical dissociation of CO₃* into O* and CO₂(g), respectively. As shown in Equation (1), the adsorption of a carbonate ion is anticipated to involve nearly a two-electron transfer process, indicating that CO₃* formation can become exothermic even at relatively low oxidation potentials, as the reaction free energy (in electronvolts) would decrease nearly twice the applied potential. Note that the pH dependence of the carbonate system reveals that, under acidic to neutral conditions, the concentration of H₂CO₃ and HCO₃⁻ is at its maximum, while CO₃²⁻ is nearly zero.^[31] This

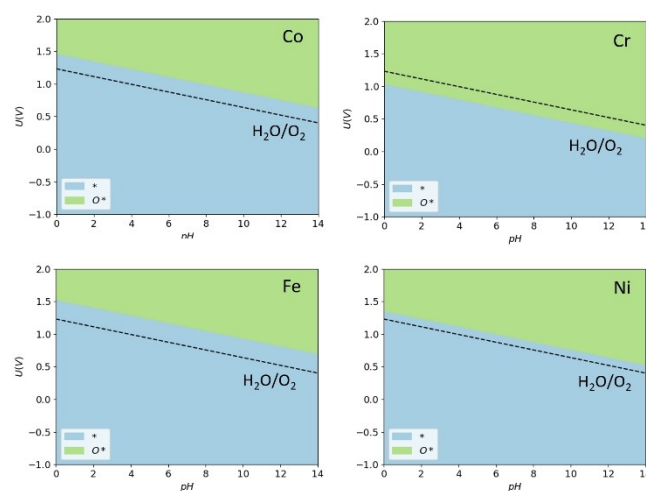


Figure 1. Pourbaix diagrams of surface adsorbed species (O*, OH*) on various metallic sites of the (CoCrFeMnNi)₃O₄ (001) surface. The dashed lines indicate the equilibrium potential for OER on the V_{RHE} scale.

phenomenon is reflected in our free energy calculations: at pH = 0, HCO_3^* formation is exothermic, whereas CO_3^* is endothermic (Table S1). Therefore, it becomes necessary to consider a pH = 12, where CO_3^{2-} concentrations are higher, in order to better align with the expected thermodynamic behavior.

To compare the formation of O^* on CCFMNO HEO from H_2O and CO_3^{2-} ions, we calculated the free energy profiles for OER and CO_3^{2-} adsorption and subsequent dissociation mechanisms (Figure S3 and Table S2). The OER free energy profile indicates that the OOH^* formation ($\text{O}^* \rightarrow \text{OOH}^*$) step acts as the potential-determining step (PDS) for all sites, including Co, Cr, Fe, and Ni, with limiting potentials of 2.28 eV, 3.41 eV, 1.72 eV, and 2.56 eV, respectively. While the O^* generation occurs within a potential range of 1.40 to 1.94 eV. This suggests that O^* formed on various sites of CCFMNO HEO is highly stable and generally does not undergo O_2 evolution under the experimental reaction conditions.

The free energies for O^* formation from CO_3^{2-} are detailed in Table S2. Note that the energy of carbonate species were obtained using thermodynamic cycles due to the challenge in directly calculating the energy of CO_3^{2-} solvated by water (Supplementary note 1, Figure S5). In the case CO_3^{2-} ions as oxidant, an applied potential of $1.5 V_{\text{RHE}}$ facilitates the generation of O^* from CO_3^{2-} ions on all metal active sites of the CCFMNO HEO surface except Ni, owing to a high CO_3 dissociation barrier. Notably, under the experimental conditions for methane activation ($1.5 V_{\text{RHE}}$ and pH = 12), O^* is preferentially forms on CCFMNO HEO, and no promotion of OER is observed. This suggests that O^* generated from CO_3^{2-} ions does not undergo further oxidation into O_2 gas; instead, it actively participates in methane activation. Therefore, carbonate ions prove to be suitable oxidant for generating O^* on the CCFMNO HEO surface.

Partial Methane Oxidation to Methanol

Figure 2a shows the calculated minimum energy pathway for methane oxidation to methanol by O^* at different metallic sites of CCFMNO HEO at $0 V_{\text{RHE}}$, pH = 12, and $T = 298 \text{ K}$. We can see that CO_3^{2-} adsorption on Co and Fe sites can become exothermic under the experimental anodic potential of approximately $1.5 V_{\text{RHE}}$ (Figure 2b). The energy barriers for the subsequent dissociation of CO_3^* into O^* and $\text{CO}_2(\text{g})$ are surmountable for Co site with a barrier of 0.73 eV and slightly higher for the Fe site, which is 0.90 eV. Meanwhile, according to Pourbaix analysis, at $1.5 V_{\text{RHE}}$ Cr and Ni sites are pre-occupied by O^* from water oxidation. Therefore, we elucidate the methane oxidation to methanol reaction mechanism from methane activation on O^* (Figure 2c).

Next step involves methane activation on O^* to produce methanol via the following reactions:

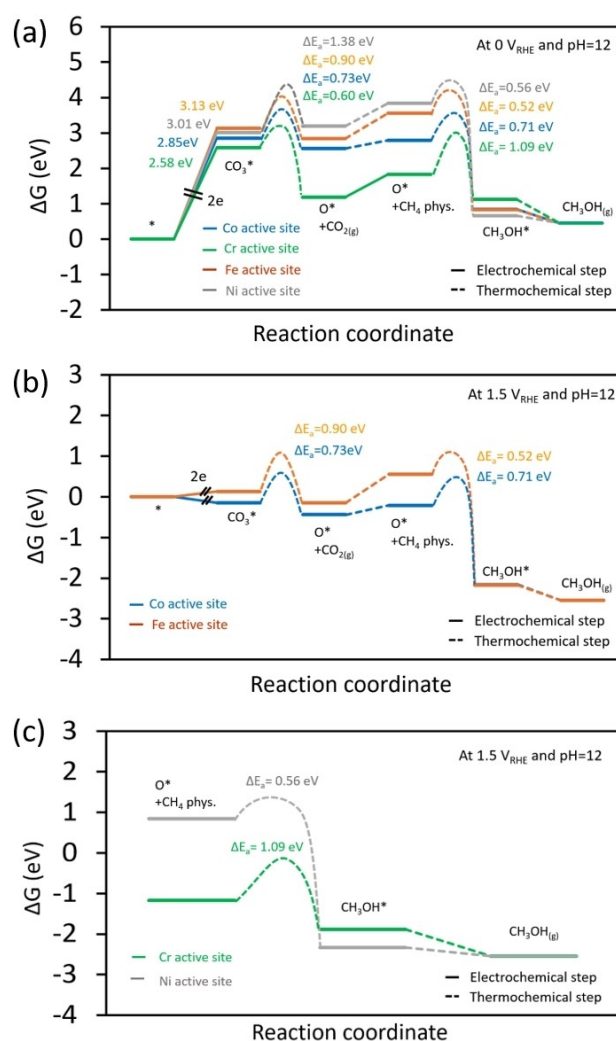
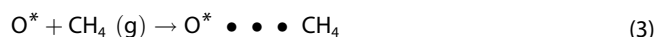


Figure 2. Free energy diagram for partial methane oxidation to methanol on (a) various metallic sites of the $(\text{CoCrFeMnNi})_3\text{O}_4$ (001) surface at $0 V_{\text{RHE}}$, pH = 12, and 298 K, (b) Co and Fe sites of the $(\text{CoCrFeMnNi})_3\text{O}_4$ (001) surface at $1.5 V_{\text{RHE}}$, pH = 12, and 298 K, (c) Cr and Ni sites of the $(\text{CoCrFeMnNi})_3\text{O}_4$ (001) surface at $1.5 V_{\text{RHE}}$, pH = 12, and 298 K.



The C–H activation barriers for the Co and Fe site are 0.71 and 0.52 eV, respectively, making them surmountable under ambient conditions. However, for the Cr site, the C–H activation barrier is 1.09 eV, making it not very surmountable under ambient conditions. Typically, an activation energy below 0.8 eV is considered kinetically viable at ambient temperature. Nevertheless, the diffusion of intermediates on the Cr site to the neighboring Co site might be possible, whereas diffusion to Fe and Ni sites is hindered by an energy difference of more than 1 eV. Therefore, Cr sites are considered unfavorable for methane oxidation. While C–H activation barrier is found to be surmountable for Ni sites, the limiting potential for O^* formation is 1.94 eV, relatively higher than the typical applied potential for methane oxidation. Overall, these findings suggest that the Co is the most active site which exhibits sufficient reactivity for C–H activation, followed by Fe in the production of methanol.

Deep Oxidation of Methanol to Ethanol and CO₂

Given relatively high limiting potential for O* formation on Ni sites (Figure 2a), and O*-assisted methane activation barrier for the Cr (Figure 2c) and we will now focus on only the Co and Fe sites, and evaluate the potential issue of the further oxidation of methanol to ethanol and CO₂ gas. The CH₃OH* deprotonation occurs via the cleavage of either the C–H bond to produce CH₂OH* or the O–H bond to produce CH₃O*.^[32] We found that CH₂OH* is much more stable than CH₃O* over Co and Fe active sites. To achieve high methanol selectivity, CH₃OH* desorption must be more favorable than the deprotonation of CH₃OH* to CH₂OH*. However, the CH₂OH* formation is exothermic than CH₃OH* desorption, i.e., $\Delta G = -0.48$ eV and -0.23 eV over Co and Fe active sites, respectively (Figure 3). This suggests that beyond methanol, CCFMNO HEO would thermodynamically favor the generation of additional oxygenated derivatives. The CH₂OH* undergoes deprotonation through an electrochemical pathway, leading to the formation of CH₂O*. Next, CH₂O* may undergo direct coupling with methane through a C–C coupling pathway to yield ethanol (CH₂O* + CH₄ → CH₃CH₂OH*), or it may further deprotonate to CHO* to ultimately yield CO₂ gas. Both pathways are regarded as viable for both the Co and Fe sites, albeit the latter route exhibits considerably greater exothermicity than the former. However, a more accurate evaluation of the product selectivity between ethanol and CO₂ gas would require a comparison between the thermochemical barrier for C–C coupling and the electrochemical barrier for CH₂OH* deprotonation, a task beyond the scope of this study. It's worth noting that accurately calculating the energy of the transition state for the C–C coupling barrier, which would resemble a methyl radical interacting with CH₂OH*, is challenging due to the complex solvation of the methyl radical in aqueous environment. The calculation of electrochemical barriers also lies beyond the scope of this present study. Consequently, this poses a challenge in conclusively determining the dominant product on this catalyst based solely on thermodynamics. Nevertheless, it's evident that CCFMNO HEO shows significant potential for producing methanol and ethanol, along with CO₂ gas. It is also quite interesting to find that CHO* deprotonation does not lead to CO* formation; instead, it results in CO₂ production through coupling with

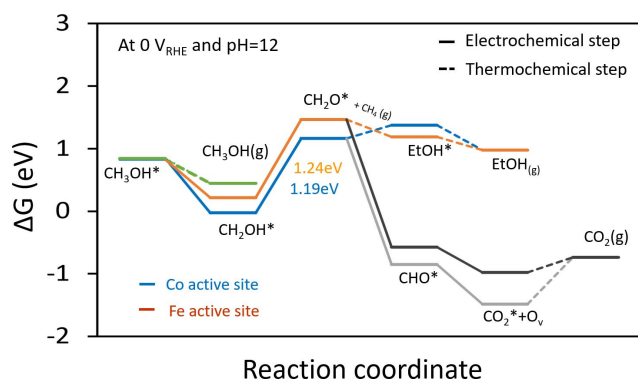


Figure 3. Free energy diagram for deep oxidation of methanol to ethanol and CO₂ on different metallic sites of the (CoCrFeMnNi)₃O₄ (001) surface at 298 K and pH = 12.

surface oxygen to yield a surface oxygen vacancy (O_v). Therefore, it is crucial to emphasize the impact of surface oxygen vacancies (O_v) on the catalyst, which can lead to the leaching of surface cations if the rate of oxygen insertion from the aqueous electrolyte is not sufficiently rapid.^[33] Given that metal leaching can significantly affect long-term stability and catalytic performance, we stress the importance of further experimental investigations to evaluate and address potential leaching effects for the practical applications of CCFMNO HEO.

Scaling and Brønsted–Evans–Polanyi Relations on CCFMNO HEO

Figure S4 exhibits a linear scaling relation observed between the adsorption energies of O* and various intermediates involved in the methane oxidation reaction, including CO₃*, CH₃OH*, CH₂OH*, CH₂O*, and CH₃CH₂OH*. This scaling relationship arises due to the shared adsorption site symmetries of O* and these intermediates. Our findings align with previous reports, notably Saidi *et al.* reported similar local scaling relationships between hydrogen-containing molecules *AH_x and *A for A = C, N, O, and S on the CoMoFeNiCu HEA surface, particularly evident when *A and *AH_x share identical adsorption site symmetry.^[34] It's important to emphasize that these observed scaling relationships are not universally applicable, unlike the scenario on uniform surfaces. Instead, these relationships hold true only when *O within reaction intermediates occupies an identical adsorption site as *O on HEOs. This observation is consistent with the results outlined by Rossmeisl on IrPdPtRhRu HEA surfaces.^[35] Hence, the energetics of all reaction steps in partial methane oxidation can be determined as a function of the adsorption energies of O* on the CCFMNO HEO surface.

Rossmeisl *et al.* reported that the Brønsted–Evans–Polanyi (BEP) relations for O₂ dissociation on HEAs do not hold due to the distinct interaction of the bound state (E_{IS}/E_{FS}) and the transition state (E_{TS}) with a different number of surface atoms.^[35] To validate this observation within the scope of CCFMNO HEO, our study focused on computing the barrier for C–H activation, a crucial step in the partial methane oxidation to methanol. In the case of CCFMNO HEO, we observed that methane activation proceeds via a radical-like TS. In addition to the conventional BEP relationship,^[36] Latimer *et al.* demonstrated that the hydrogen affinity (ΔE_{OH*}–ΔE_{O*}) serves as an effective descriptor for C–H activation that proceeds through a radical-like TS.^[37] Our findings, illustrated in Figure 4 (a), reveal a positive linear correlation between E_{TS} and ΔE_{OH*}–ΔE_{O*}. This indicates that higher proton affinity facilitates more facile C–H activation. Consequently, while BEP relations are applicable on CCFMNO HEO, employing a descriptor that considers the local structure of the E_{IS}/E_{FS} and E_{TS} is crucial for their accurate interpretation.

Origins of Catalytic Activity through Electronic Structure

We investigated the electronic structure of CCFMNO HEO to explore the origin of catalytic activity in the partial oxidation of

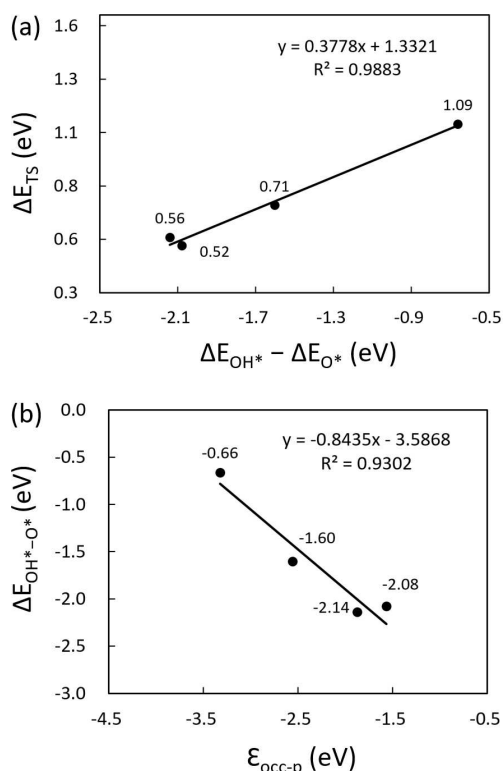


Figure 4. (a) Brønsted–Evans–Polanyi relations on $(\text{CoCrFeMnNi})_3\text{O}_4$ (001) surface: The energy barrier for methane C–H bond activation (ΔE_{TS}) as a function of $\Delta E_{\text{OH}^*} - \Delta E_{\text{O}^*}$ (eV). (b) Electronic structure descriptor revealing the proton affinity ($\Delta E_{\text{OH}^*} - \Delta E_{\text{O}^*}$) in relation to the occupied p-band center ($\epsilon_{p\text{-occ}}$) of the active oxygen.

methane. Traditionally, the d-band center of transition metals serves as a measure of intermediate adsorption energy.^[38] Considering the direct interaction of O^* in C–H activation, we proceeded to calculate the occupied p-band center ($\epsilon_{p\text{-occ}}$) of O^* (Figure 4b, refer to Supplementary note 2 and Table S3 for detailed values). The $\epsilon_{p\text{-occ}}$ exhibits a negative correlation with proton affinity, displaying a strong correlation with an R^2 value of 0.93. A more positive $\epsilon_{p\text{-occ}}$ signifies a higher energy level of the 2p orbital in oxygen, leading to a more active O^* and improved proton affinity. Consequently, utilizing the occupied p-band center of O^* can serve as an effective electronic descriptor. These correlations highlight potential catalyst design strategies, emphasizing the significance of electronic structure in governing methane conversion catalytic activity.

Conclusions

Our study highlights the important role of CO_3^{2-} ions in generating active oxygen species (O^*) essential for electrochemical methane oxidation to alcohols on CCFMNO HEO surfaces. Among various active sites of $(\text{CoCrFeMnNi})_3\text{O}_4$, we identify Co as the most active for methane activation, yielding methanol with a limiting potential of 1.4 V, and ethanol and CO_2 with a limiting potential of 1.2 V. We have also shown that the linear scaling and BEP relations do hold on HEOs, contrary to the

disagreement in previous reports on HEAs. Furthermore, we have established robust linear correlations between occupied p-band centers and proton affinity, directly influencing C–H activation—a crucial step in methane conversion. In summary, our findings elucidate key mechanistic pathways and catalyst design principles for efficient partial methane oxidation on CCFMNO HEO, providing valuable insights for future catalyst development.

Computational Details

Spin-polarized DFT calculations were performed using the Vienna Ab initio Simulation Package (VASP) with the Atomistic Simulation Environment (ASE).^[39,40] The interactions between electrons and ion cores were described by the projector augmented wave (PAW) potential. The exchange and correlation energy was described by the revised Perdew–Burke–Ernzerhof (GGA–RPBE) functionals.^[41,42] We employed the rotationally invariant form of the DFT+U approach proposed by Dudarev *et al* to account for Coulomb correlation effect.^[43] We set U_{eff} ($U_{\text{eff}} = U - J$) for transition metals, $U_{\text{eff}} = 3.32, 3.70, 5.30, 3.90, 6.20$ eV for Co, Cr, Fe, Mn, Ni, respectively. A kinetic energy cutoff of 500 eV was used for plane-wave expansion. Monkhorst–Pack k -point meshes of $4 \times 4 \times 1$ were used for all slab calculations. During structural optimization, the energy and force convergence criteria were set to 10^{-5} eV and 0.3 eV/Å, respectively. The climbing image nudged elastic band (CI–NEB) method was used to calculate the transition-state (TS) geometries.^[44]

Supporting Information

The authors have cited additional references within the Supporting Information (Ref. [45,46,55,47–54]).

Acknowledgements

This work was supported by the National Research Foundation of Korea (NRF) grant funded by the Ministry of Science and ICT, Korea government (No. 2022M3C1A3096454) for M.R.A.K. and S.W.L.. J.S.Y. acknowledges the support from the 2023 Research Fund of the University of Seoul. DFT calculations were performed using the computational resources in the Urban Big data and AI Institute (UBAI) of the University of Seoul.

Conflict of Interests

The authors declare no conflict of interest.

Data Availability Statement

The data that support the findings of this study are available from the corresponding author upon reasonable request.

Keywords: high-entropy oxides · methane oxidation · electrocatalysis · density functional theory · alcohols

- [1] R. A. Kerr, *Sci. Mag.* **2010**, *328*, 1624.
- [2] D. Saha, H. A. Grappe, A. Chakraborty, G. Orkoulas, *Chem. Rev.* **2016**, *116*, 11436.
- [3] T. Ma, Q. Fan, X. Li, J. Qiu, T. Wu, Z. Sun, *J. CO₂ Util.* **2019**, *30*, 168.
- [4] S. D. Lacey, Q. Dong, Z. Huang, J. Luo, H. Xie, Z. Lin, D. J. Kirsch, V. Vattipalli, C. Povinelli, W. Fan, R. Shahbazian-Yassar, D. Wang, L. Hu, *Nano Lett.* **2019**, *19*, 5149.
- [5] X. Chen, C. Si, Y. Gao, J. Frenzel, J. Sun, G. Eggeler, Z. Zhang, *J. Power Sources* **2015**, *273*, 324.
- [6] M. W. Glasscott, A. D. Pendergast, S. Goines, A. R. Bishop, A. T. Hoang, C. Renault, J. E. Dick, *Nat. Commun.* **2019**, *10*, 2650, DOI 10.1038/s41467-019-10303-z.
- [7] H. J. Qiu, G. Fang, Y. Wen, P. Liu, G. Xie, X. Liu, S. Sun, *J. Mater. Chem. A* **2019**, *7*, 6499.
- [8] G. Zhang, K. Ming, J. Kang, Q. Huang, Z. Zhang, X. Zheng, X. Bi, *Electrochim. Acta* **2018**, *279*, 19.
- [9] Y. Yao, Z. Huang, P. Xie, S. D. Lacey, R. J. Jacob, H. Xie, F. Chen, A. Nie, T. Pu, M. Rehwoldt, D. Yu, M. R. Zachariah, C. Wang, R. Shahbazian-Yassar, J. Li, L. Hu, *Science* **2018**, *359*, 1489.
- [10] P. Xie, Y. Yao, Z. Huang, Z. Liu, J. Zhang, T. Li, G. Wang, R. Shahbazian-Yassar, L. Hu, C. Wang, *Nat. Commun.* **2019**, *10*, 1.
- [11] A. L. Wang, H. C. Wan, H. Xu, Y. X. Tong, G. R. Li, *Electrochim. Acta* **2014**, *127*, 448.
- [12] C. F. Tsai, K. Y. Yeh, P. W. Wu, Y. F. Hsieh, P. Lin, *J. Alloys Compd.* **2009**, *478*, 868.
- [13] S. Nellaiappan, N. K. Katiyar, R. Kumar, A. Parui, K. D. Malviya, K. G. Pradeep, A. K. Singh, S. Sharma, C. S. Tiwary, K. Biswas, *ACS Catal.* **2020**, *10*, 3658.
- [14] J. K. Pedersen, T. A. A. Batchelor, A. Bagger, J. Rossmeisl, *ACS Catal.* **2020**, *10*, 2169.
- [15] V. A. Mints, J. K. Pedersen, A. Bagger, J. Quinson, A. S. Anker, K. M. Ø. Jensen, J. Rossmeisl, M. Arenz, *ACS Catal.* **2022**, *12*, 11263.
- [16] J. K. Pedersen, T. A. A. Batchelor, D. Yan, L. E. J. Skjægstad, J. Rossmeisl, *Curr. Opin. Electrochem.* **2021**, *26*, 100651.
- [17] C. M. Rost, E. Sacht, T. Borman, A. Moballegh, E. C. Dickey, D. Hou, J. L. Jones, S. Curtarolo, J. P. Maria, *Nat. Commun.* **2015**, *6*, 8485, DOI 10.1038/ncomms9485.
- [18] B. Cantor, I. T. H. Chang, P. Knight, A. J. B. Vincent, *Mater. Sci. Eng. A* **2004**, *375–377*, 213.
- [19] M. C. Tropaevsky, J. R. Morris, P. R. C. Kent, A. R. Lupini, G. M. Stocks, *Phys. Rev. X* **2015**, *5*, 1.
- [20] D. Ma, B. Grabowski, F. Körmann, J. Neugebauer, D. Raabe, *Acta Mater.* **2015**, *100*, 90.
- [21] T. Löffler, H. Meyer, A. Savan, P. Wilde, A. Garzón Manjón, Y. T. Chen, E. Ventosa, C. Scheu, A. Ludwig, W. Schuhmann, *Adv. Energy Mater.* **2018**, *8*, 1.
- [22] C. Triolo, K. Moulae, A. Ponti, G. Pagot, V. Di Noto, N. Pinna, G. Neri, S. Santangelo, *Adv. Funct. Mater.* **2024**, *34*, 2306375, DOI 10.1002/adfm.202306375.
- [23] C. Triolo, S. Schweidler, L. Lin, G. Pagot, V. Di Noto, B. Breitung, S. Santangelo, *Energy Adv.* **2023**, *2*, 667, DOI 10.1039/d3ya00062a.
- [24] Z. Sun, Y. Zhao, C. Sun, Q. Ni, C. Wang, H. Jin, *Chem. Eng. J.* **2022**, *431*, 133448.
- [25] M. Einert, M. Mellin, N. Bahadorani, C. Dietz, S. Lauterbach, J. P. Hofmann, *ACS Appl. Energy Mater.* **2022**, *5*, 717.
- [26] S. H. Albedwawi, A. AlJaberi, G. N. Haidemenopoulos, K. Polychronopoulou, *Mater. Des.* **2021**, *202*, 109534.
- [27] A. Van De Walle, P. Tiwary, M. De Jong, D. L. Olmsted, M. Asta, A. Dick, D. Shin, Y. Wang, L. Q. Chen, Z. K. Liu, *CALPHAD Comput. Coupling Phase Diagrams Thermochem* **2013**, *42*, 13.
- [28] M. R. A. Kishore, S. Lee, J. S. Yoo, *Adv. Sci.* **2023**, *10*, 2301912.
- [29] C. Kim, H. Min, J. Kim, J. Sul, J. Yang, J. H. Moon, *Appl. Catal. B* **2023**, *323*, 122129.
- [30] J. Lee, J. Yang, J. H. Moon, *ACS Energy Lett.* **2021**, *6*, 893.
- [31] J. Zosel, W. Oelner, M. Decker, G. Gerlach, U. Guth, *Meas. Sci. Technol.* **2011**, *22*, 072001, DOI 10.1088/0957-0233/22/7/072001.
- [32] J. H. M. Jaehyun Lee, S. Lee, C. Kim, J. S. Yoo, *Appl. Catal. B Environ. Energy* **2024**, *344*, 123633, DOI 10.1016/j.apcatb.2023.123633.
- [33] J. Wang, S. Sun, S. Xi, Y. Sun, S. J. H. Ong, Z. W. Seh, Z. J. Xu, *J. Phys. Chem. C* **2024**, *128*, 4978, DOI 10.1021/acs.jpcc.4c00670.
- [34] J. Zhang, C. Cai, G. Kim, Y. Wang, W. Chen, *npj Comput. Mater.* **2022**, *8*, 1.
- [35] K. L. Svane, J. Rossmeisl, *Angew. Chemie–Int. Ed.* **2022**, *61*, e202201146, DOI 10.1002/anie.202201146.
- [36] T. Bligaard, J. K. Nørskov, S. Dahl, J. Matthiesen, C. H. Christensen, J. Sehested, *J. Catal.* **2004**, *224*, 206.
- [37] A. A. Latimer, A. R. Kulkarni, H. Aljama, J. H. Montoya, J. S. Yoo, C. Tsai, F. Abild-Pedersen, F. Studt, J. K. Nørskov, *Nat. Mater.* **2017**, *16*, 225.
- [38] B. Hammer, J. K. Nørskov, *Surf. Sci.* **1995**, *343*, 211.
- [39] G. Kresse, J. Furthmüller, *Comput. Mater. Sci.* **1996**, *6*, 15.
- [40] A. Hjorth Larsen, J. Jørgen Mortensen, J. Blomqvist, I. E. Castelli, R. Christensen, M. Duřak, J. Friis, M. N. Groves, B. Hammer, C. Hargus, E. D. Hermes, P. C. Jennings, P. Bjerre Jensen, J. Kermode, J. R. Kitchin, E. Leonhard Kolsbjerg, J. Kubal, K. Kaasbjerg, S. Lysgaard, J. Bergmann Maronsson, T. Maxson, T. Olsen, L. Pastewka, A. Peterson, C. Rostgaard, J. Schiøtz, O. Schütt, M. Strange, K. S. Thygesen, T. Vegge, L. Vilhelmsen, M. Walter, Z. Zeng, K. W. Jacobsen, *J. Phys. Condens. Matter* **2017**, *29*, 273002, DOI 10.1088/1361-648X/aa680e.
- [41] B. Hammer, L. B. Hansen, J. K. Nørskov, *Phys. Rev. B: Condens. Matter Phys.* **1999**, *59*, 7413.
- [42] J. P. Perdew, K. Burke, M. Ernzerhof, *Phys. Rev. Lett.* **1996**, *77*, 3865.
- [43] S. L. Dudarev, G. A. Botton, S. Y. Savrasov, C. J. Humphreys, A. P. Sutton, *Phys. Rev. B* **1998**, *57*, 1505.
- [44] G. B. P. U. H. J. Henkelman, *J. Chem. Phys.* **2000**, *113*, 9901.
- [45] F. Gossenberger, T. Roman, A. Groß, *Electrochim. Acta* **2016**, *216*, 152.
- [46] I. T. McCrum, S. A. Akhade, M. J. Janik, *Electrochim. Acta* **2015**, *173*, 302.
- [47] H. A. Hansen, I. C. Man, F. Studt, F. Abild-Pedersen, T. Bligaard, J. Rossmeisl, *Phys. Chem. Chem. Phys.* **2010**, *12*, 283.
- [48] L. P. Granda-Marulanda, I. T. McCrum, M. T. M. Koper, *J. Phys. Condens. Matter* **2021**, *33*, 204001, DOI 10.1088/1361-648X/abf19d.
- [49] F. Calle-Vallejo, M. Huang, J. B. Henry, M. T. M. Koper, A. S. Bandarenka, *Phys. Chem. Chem. Phys.* **2013**, *15*, 3196.
- [50] R. Christensen, H. A. Hansen, T. Vegge, *Catal. Sci. Technol.* **2015**, *5*, 4946.
- [51] A. A. Peterson, F. Abild-Pedersen, F. Studt, J. Rossmeisl, J. K. Nørskov, *Energy Environ. Sci.* **2010**, *3*, 1311.
- [52] F. Studt, F. Abild-Pedersen, J. B. Varley, J. K. Nørskov, *Catal. Lett.* **2013**, *143*, 71.
- [53] L. P. Granda-Marulanda, A. Rendón-Calle, S. Builes, F. Illas, M. T. M. Koper, F. Calle-Vallejo, *ACS Catal.* **2020**, *10*, 6900.
- [54] J. K. Nørskov, J. Rossmeisl, A. Logadottir, L. Lindqvist, J. R. Kitchin, T. Bligaard, H. Jónsson, *J. Phys. Chem. B* **2004**, *108*, 17886.
- [55] F. Boca Raton, *CRC Handbook of Chemistry and Physics, 87th Ed* Editor-in-Chief: David R. Lide (National Institute of Standards and Technology). CRC Press/Taylor and Francis Group: Boca Raton, FL, **2006**, 2608.

Manuscript received: January 31, 2024

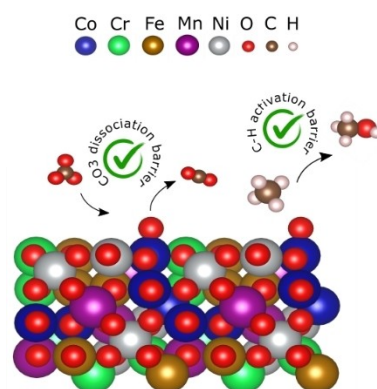
Revised manuscript received: March 28, 2024

Accepted manuscript online: March 28, 2024

Version of record online: ■■, ■■

RESEARCH ARTICLE

This research explores the potential of $(\text{CoCrFeMnNi})_3\text{O}_4$ high-entropy oxides for electrochemical methane oxidation to methanol, ethanol, along with CO_2 gas. The study reveals correlations between occupied p-band centers and proton affinity, influencing the crucial C–H activation in methane conversion. These insights contribute to catalyst design principles for enhancing partial methane oxidation efficiency on high-entropy oxides.



*Dr. M. R. A. Kishore, S. Lee, Prof. J. S. Yoo**

1 – 7

A Density Functional Theory Analysis of Electrochemical Oxidation of Methane to Alcohol over High-Entropy Oxide $(\text{CoCrFeMnNi})_3\text{O}_4$ Catalysts

